Hindawi Complexity Volume 2021, Article ID 5616826, 12 pages https://doi.org/10.1155/2021/5616826



## Research Article

# **Virtual Reconstruction Method of Regional 3D Image Based on Visual Transmission Effect**

# Jing Yin (b)1,2 and Jong Hoon Yang<sup>2</sup>

<sup>1</sup>College of Media and Design, Chongqing Technology and Business Institute, Chongqing Radio & TV University, Chongqing 400052, China

Correspondence should be addressed to Jing Yin; yinjingcq11@cumt.edu.cn

Received 16 April 2021; Revised 27 May 2021; Accepted 5 June 2021; Published 12 June 2021

Academic Editor: Zhihan Lv

Copyright © 2021 Jing Yin and Jong Hoon Yang. This is an open access article distributed under the Creative Commons Attribution License, which permits unrestricted use, distribution, and reproduction in any medium, provided the original work is properly cited.

In order to solve the problems of poor user experience and low human-computer interaction efficiency, this paper designs a 3D image virtual reconstruction system based on visual communication effects. First, the functional framework diagram and hardware structure diagram of the image 3D reconstruction system are given. Then, combined with the basic theory of visual communication design, the characteristics of different elements in the three-dimensional image system and reasonable visual communication forms are analyzed, and design principles are proposed to improve user experience and communication efficiency. After the input image is preprocessed by median filtering, a three-dimensional reconstruction algorithm based on the image sequence is used to perform a three-dimensional reconstruction of the preprocessed image. The performance of the designed system was tested in a comparison form. We optimize the original hardware structure, expand the clock module, and use the chip to improve the data processing efficiency; in the two-dimensional image; we read the main information, through data conversion, display it in three-dimensional form, select the feature area, extract the image feature, calculate the key physical coordinate points, complete the main code compilation, use visual communication technology to feed back the display visual elements to the 3D image, and complete the design of the 3D image virtual reconstruction system. The test results showed that the application of visual communication technology to the virtual reconstruction of 3D images can effectively remove noise and make the edge area of the image clear, which can meet the needs of users compared with the reconstruction results of the original system. Visual C++ and 3DMAX are used as the system design platform, and three-dimensional image visualization and roaming are realized through OpenGL. Experimental results show that the designed system has better reconstruction accuracy and user satisfaction.

#### 1. Introduction

With the advent of the digital age, digital imaging technology continues to improve, and digital images are widely used. A digital image can also be called a digital image, which is a kind of digital image, which is essentially a two-dimensional matrix, and each point in the matrix is called a pixel [1]. A digital image is a representation of a two-dimensional image with limited digital value pixels. It is represented by an array or matrix, and its light position and intensity are all discrete. A digital image is an image that is obtained by digitizing an analog image with pixels as the

basic element and can be stored and processed by a digital computer or digital circuit. Visual communication technology is a highly comprehensive composite technology, mainly involving computer modeling technology, human-computer interaction technology, sensors, graphics and image processing technology, and simulation technology [2]. Visual communication technology can affect not only the user's visual experience but also nonvisual experiences such as hearing, touch, and force. At this stage, visual communication technology has been widely used in the fields of medicine, education, military, and culture [3]. The image-based 3D reconstruction algorithm is a key

<sup>&</sup>lt;sup>2</sup>Department of Digital Image, Graduate School of Sangmyung University, Seoul 03016, Republic of Korea

technology of visual communication technology, and it is also a hot topic of recent research [4].

Most of the current digital images use three-dimensional images. When converting a two-dimensional plane image into a three-dimensional image, the work is usually done by modeling, but the image is often incomplete or damaged, so it needs to be reconstructed [5]. In previous studies, some scholars have designed reconstruction systems for 3D digital images, but in the process of use, the image will be distorted and incomplete. The ultimate goal of 3D reconstruction is to be able to reconstruct any 3D shape from any image. However, learning-based techniques only perform well on images and objects in the training set. An interesting direction for future research is to combine traditional techniques with learning-based techniques to improve the generalization ability of the latter method. At present, most of the 3D image reconstruction systems based on visual communication technology focus on the use of more advanced equipment or more advanced reconstruction algorithms, while ignoring the problems of user experience quality and human-computer interaction efficiency [6]. In addition, the design principle of the traditional two-dimensional graphical user interface is the concept of planarization, which has been unable to meet the needs of interactive experience in three-dimensional space, and cannot provide better visual communication and interactive experience [7]. Some documents have conducted detailed studies on the evolution of two-dimensional animation and three-dimensional animation in visual communication, verifying the feasibility and applicability of the principle of visual communication in three-dimensional graphic design [8].

Visual communication technology covers multimedia technology and image technology, etc., and has been widely used in different fields. Based on this, this paper designs a three-dimensional image reconstruction system based on visual communication technology, builds a three-dimensional image reconstruction system on the basis of the image processing system, uses visual communication technology to process the image, selects the characteristic points related to the three-dimensional image in the image, and realizes the three-dimensional image reconstruction. By setting visual symbols in the images, they are conveyed to the viewer through the designer's thoughts, so that the viewer becomes the audience of the designer's thoughts. The use of visual communication technology is of great assistance to the reconstruction of the details of the three-dimensional image. In this research, the visual communication technology part of the reconstruction system will be reoptimized and designed to provide a basis for the realization of system performance. First, the system function framework of 3D image reconstruction is analyzed, and then the main submodules of the system which are the image analysis module, image preprocessing module, and 3D visualization module are designed in detail. Finally, simulation comparisons with traditional 3D image reconstruction systems are carried out in the same environment of the experiment. This paper designs a three-dimensional image reconstruction system based on visual communication technology, constructs a

three-dimensional image reconstruction system on the basis of the image processing system, uses visual communication technology to process images, selects characteristic points related to the three-dimensional image in the image, and realizes the three-dimensional image reconstruction. The experimental results show that the 3D image reconstruction based on visual communication technology has high accuracy and improves the efficiency of 3D image reconstruction. The overall effect of 3D image reconstruction is significantly better than traditional 3D image reconstruction systems and has higher practical application value.

## 2. Related Work

The realization method based on visual communication effect is simple to operate and easy to realize. It has an irreplaceable role in noncontact three-dimensional measurement, robot guidance, visual communication, local operating system position measurement, and control [9]. Many scholars at home and abroad have conducted research on binocular vision, and the three-dimensional reconstruction of binocular vision is an important aspect, mainly studying the two parts of stereo matching and three-dimensional reconstruction methods [10].

Through the 3D scene modeling and analysis of the pictures on the Internet, 3D point cloud information can be obtained, so as to realize the 3D reconstruction of the scene in the picture. The system is very effective for the reconstruction of some famous sites [11]. The University of Washington has also cooperated with Microsoft Corporation. Gibbs [12] developed a wide-baseline stereo vision system to provide three-dimensional information within a few kilometers on Mars for the "Surfer" and install the same camera at different positions of the detector to collect the terrain. The larger the distance between the cameras is, the wider the baseline is and the longer the measurement distance is. In order to obtain the relative position of the images collected at different times, nonlinearity is adopted. The method optimizes the system. In order to make the matching disparity map reach the subpixel level, the maximum likelihood method and stereo search are combined for image matching, and finally, the three-dimensional coordinates of each matching point are calculated according to the disparity map. Based on the characteristics of servo robots, Xu et al. [13] developed an adaptive visual communication effect system. The system used stereo parallax as the basic principle and used relatively static points in the two images as reference points to calculate the image. The real-time Jacobian matrix uses this known information to predict the nextmoment action of the target in the image. The prediction result of the system is more accurate, so it has a prominent role in adaptive target tracking. Compared with the traditional visual tracking system, the system does not need to calculate the camera's optical and motion parameters, which greatly improves the real-time efficiency of the system. Leung and Malik [14] used the principle of triangulation to apply binocular vision technology to the human body on some occasions. In the measurement, the problem of human measurement in these occasions is solved; for example, some

tourists and passengers need to be measured in entertainment venues and in the process of riding a car. De Reu et al. [15] applied the graph cut theory to the calculation of the energy function, solved its minimization problem, and then provided a theoretical basis for multiview computer vision 3D reconstruction. This three-dimensional reconstruction method based on the graph cut method is to construct a binary variable function and then calculate it to achieve three-dimensional reconstruction. In terms of computing speed, graphics visualization, etc., it is significantly better than traditional algorithms.

Compared with foreign countries, the research on binocular vision technology is a bit late, but it does not mean that the development is slow after the start. We have moved from slow imitation to independent innovation. A large number of scientific and technological talents have invested in this area. In terms of research, great progress has also been made in visual processing. This technology has been applied in many fields in China. Park et al. [16] proposed a 3D point cloud reconstruction method for human faces using binocular vision. This method improved the matching link in 3D reconstruction, increasing the original matching to two times. The first is the seed point algorithm is used for rough matching, then, the area near the rough matching point is resegmented and described, then, the description points are densely matched, and finally, a high-accuracy three-dimensional point cloud model of the face is obtained. The advantage of this method is that it improves the accuracy of the system, but at the same time, it increases the complexity of the algorithm. Leith and Upatnieks [17] have built a binocular vision system using a laser pointer and a binocular camera. The system is mainly designed for scenes with weak texture information. In fact, it uses the projection characteristics of the laser pointer to solve this problem. The entire system is mounted on the robot to help the robot quickly deal with obstacles in weak texture scenes, identify objects, and provide a basis for their autonomous path planning. The effect of this system in weak texture scenes is better, and this is also its defect. It can only be processed for specific scenes, and its portability is poor. Beijing University of Aeronautics and Astronautics uses the basic principles of stereo vision to realize the 3D reconstruction of the terrain contour. They proposed a three-dimensional reconstruction method based on region segmentation based on terrain features. First, the image was segmented using a more classic watershed algorithm, and the segmented boundary was used as the contour edge in the actual scene. Then, the global features of its adjacent segmented regions and the scale, location, and gray value distribution characteristics of each local area are used as stereo matching constraints. This method not only reduces the matching search space but also improves efficiency. This method is based on region segmentation. When observing from different viewpoints, there are certain differences in the contours seen, which will increase the matching error [18]. Harbin Institute of Technology has also done related research, which uses visual communication effect technology to identify and locate workpieces. The 3D image reconstruction method can solve the problem of single-angle image information acquisition and lack of depth

information. This method was initially mainly used in the medical field to display human tissue images through radiological medical equipment. After gradual development, it has been used in the military, surveying and mapping, aviation, etc. First, it uses the edge detection method to complete the detection of the workpiece, specifically based on the Sobel operator. Combined with the area growth, it improves the problem of the low precision of the traditional Sobel operator. Then, according to the principle of binocular parallax, the detection of the extracted edge information feature is used as the matching feature, and then, the matching is realized. Finally, the spatial pose of the workpiece is reconstructed according to the matching information. This method has a better detection effect on workpieces with clear edges. When the contours of the workpiece edges become blurred, this method will be greatly reduced [19]. Some researchers from Shandong Normal University have in-depth research on the 3D reconstruction method based on feature point matching. Based on the SIFT algorithm, the Harris corner point matching algorithm and the SIFT algorithm are combined to make the feature detection of the target reach the subpixel level, which greatly improves the traditional algorithm detected by the problem of low accuracy and finally uses the principle of parallax to calculate the three-dimensional information of the target. Although this method has high reconstruction accuracy, it still has problems such as slow calculation speed and sparse feature points [20–22].

In summary, each stereoscopic 3D reconstruction method has more or less defects. Relatively speaking, the 3D reconstruction based on feature points has good stability and high accuracy. Based on the regional 3D image virtual algorithm, this article focuses on how to improve the algorithm speed and improve the sparse feature points. In terms of improving algorithm speed, we have the following: integrating epipolar constraints into feature matching, improving matching efficiency, and saving time for the operation of the entire system; concerning solving the problem of sparse feature points, we have the following: triangulating feature points according to the circumscribed circle criterion to approximate replacement objects which greatly improves the problem of sparse feature point detection.

## 3. Construction of Regional 3D Image Virtual Model Based on Visual Communication Effect

3.1. Level Distribution of Visual Communication. The hardware part of the system is redesigned according to the characteristics of each link of digital image processing [23–26]. The main structure includes three parts: image acquisition layer, image processing layer, and image reconstruction layer. The initial data of 3D digital image reconstruction is a result of the comparison and fusion of depth data and color data collected at the same time. Corresponding color cameras are configured in the original reconstruction system. In order to ensure that the collected

initial information is suitable for visual communication technology, the depth camera is used on the original basis to complete the acquisition of depth data [27–30]. The data I/O submodule, parameter setting submodule, volume rendering submodule, surface rendering submodule, and axial slice display submodule together constitute the 3D visualization module, and its structure is shown in Figure 1.

The surface rendering submodule of the 3D visualization module uses the SMC algorithm proposed based on the MC (Marching Cubes) algorithm to reconstruct the object surface in the image. The detailed process is as follows: assuming that there are a series of contour lines related to the object in the object image, we use P1, P2,..., P-n, implement hierarchical write operation on the image data field, and define the state function u(x) of each n(x) in the volume data as

$$u(x) = \left\{ i \middle| \frac{n(x) \cdot c(i)}{1 + c(i)} > \sin x \right\},\tag{1}$$

Let V(p) be a group of photos of image I, and let  $V^*(p)$  be a group of photos filtered by the useless image threshold. The calculation methods of the two are as follows:

$$v(x) = \{i | i \in u(x), \quad h(i, j) < a\}. \tag{2}$$

In the formula, p represents the patch, h(i) and h(j) are adjustment factors, and v(x) represents the reference image of the patch p. The metric function of the three-dimensional reconstruction algorithm of p on v(x) and  $V^*(p)$  is

$$f(p) = \frac{1}{(u(x)/r(p))} * \sum h(i, j),$$
 (3)

where h(p, I, r(p)) is the metric function of the projection of p on I and r(p). In order to get a better photo group V(p), it is filtered by the following formula:

$$g(n) = \frac{r(n) \lim_{n \to \infty} \sum_{i=1}^{n} h(i, j, r(n))}{v(r) + 1},$$
 (4)

where w is the scale space factor. Setting it to increase exponentially, each value has a corresponding image, these images are formed into a Gaussian pyramid, the feature extraction of the pyramid is performed, and the extreme points are set as the feature points of the image, which are reflected through the definition of DOG, as follows:

$$w(p) = \begin{cases} 1, & p < i, \\ 0, & p \ge i. \end{cases}$$
 (5)

First, we construct a three-dimensional scale space, perform convolution operations on the Gaussian function of different scale factors and the image to form a series of images with different scales and image pixels, and set the scale space to w(p) and the original image to w(i). The Gaussian function is g(x, y). Then,

$$y(a,b) = t \int \frac{f(i,j) \cdot g(x,y)}{1 + g(x,y)} dxdy.$$
 (6)

In the formula, y(a,b) represents all the patch sets that do not meet the required visible information. We define L(x) to

represent a solid model; then, the spatial indicator function used in surface reconstruction is

$$L(x) = \int \frac{y(x)|x|}{1+x} dx.$$
 (7)

In the formula, n is the scale shrinkage factor. We find the extreme point in the result of the formula, which is the characteristic point of the image. We match the acquired feature points, calculate their consistency, get the key points of image reconstruction, and complete the 3D digital image reconstruction work. Because each vertex has three possible vertex values (+1, 0, -1), there are 38 possibilities for each voxel. Some formulas and meanings of variable symbols are shown in Table 1. Due to the symmetry of voxels, 6 561 possibilities of voxels can be simplified, and because there is no difference between the state values of the pixels and the four neighborhoods, a large number of nonexistent models are eliminated, and only 52 surface reconstruction models remain.

3.2. Regional 3D Image Virtual Algorithm. For a single voxel, according to the state value, each vertex value is any one of +1, 0, -1. Under the condition that the boundary surface passes through the vertex with a state value of 0, if the state values of the two vertices of an edge on the voxel are different, it means that the boundary surface and the edge are in an intersecting relationship; if the two vertices of an edge on the voxel are intersected, the state values are consistent, indicating that there is a disjoint relationship between the boundary surface and this edge. Under the condition that there is an intersection relationship between the boundary surface and a certain edge, considering the lack of a corresponding threshold value for the image, the intersection is implemented; at the same time, due to the high definition of the image used for 3D reconstruction, the error value is about 0.5 edge length, which is projected to the image on the computer screen which is basically the same as the image obtained by linear interpolation, so the midpoint of this edge is the intersection point. As shown in Figure 2, through the above process, the intersection point between the object surface and the voxel can be determined, and the threedimensional image can be reconstructed by connecting the intersection points in turn. The system consists of an image analysis module, an image preprocessing module, and a three-dimensional visualization module. The main function of the image analysis module is to support the reading of different original image data formats.

On the basis of the original 3D digital image reconstruction system, visual communication technology is used to ensure the feasibility of this technology in the 3D image reconstruction system. The image preprocessing module processes the original image data matrix function processing and converts the original image data into a three-dimensional data field to obtain images through visual communication technology and feature extraction technology. The specific process design is as follows: (1) after inputting the image, capture the original image; (2) preprocess the image to make the image more suitable for processing and

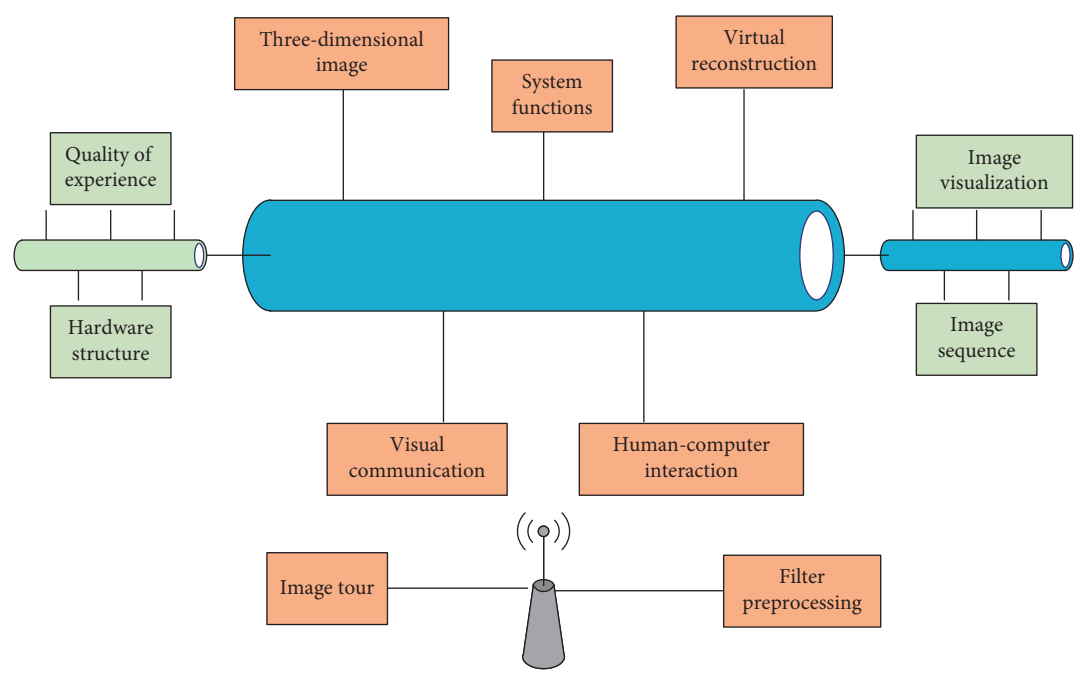


FIGURE 1: Hierarchical structure of visual communication effects.

TABLE 1: Formulas and meanings of variable symbols.

Symbol	u(x)	v(x)	f(p)	g(n)	w(p)	<i>y</i> ( <i>a</i> , <i>b</i> )	L(x)
Meaning	The state	Image	Metric function of	Metric function of	Feature extraction	Patch	Key points of image
	function	threshold	reconstruction algorithm	the projection	of the pyramid	sets	reconstruction

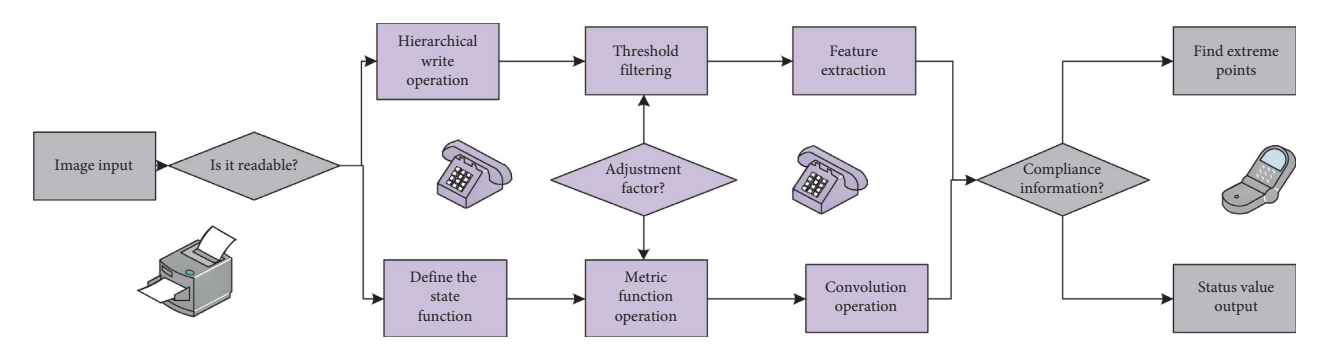


FIGURE 2: Regional 3D image virtual algorithm.

manipulation than the original image; (3) supplement the missing parts of the image space domain to enhance the original image space domain; (4) improve the appearance of the image, based on Step 3 for further optimization; (5) describe the image with different resolutions, and adapt the image to adaptively find the most suitable resolution; (6) perform image segmentation after the resolution is described; (7) complete the image processing and output a new image. The 3D image reconstruction is achieved through the above process. We set the reconstructed feature point set as u, S is the reconstructed 3D image vector, and the original image feature point is p. There is a point overlap in the reconstructed image. In order to prepare the tissue area, a three-dimensional image reconstruction system is designed based on the image using volume rendering technology and

surface rendering technology to realize the output of the three-dimensional space visualization function of the image. The coincidence part is not included in the accuracy calculation.

3.3. Optimization of the 3D Image Virtual Model. The frame diagram of the virtual reconstruction of 3D images based on visual communication is shown in Figure 3. In the image acquisition stage, due to the influence of external imaging equipment and the surrounding environment, the images imported into the system have a certain degree of noise and blur, which affects the effect of 3D image reconstruction. Therefore, it is necessary to adopt image preprocessing techniques such as filtering, segmentation, and registration

to enhance image characteristics. Taking into account the filtering effect and operating efficiency, the median filtering method is used in the image filtering process: a window with an odd number of pixels is set on the original image, and the pixels contained in this window are sorted according to the size, and the middle gray value of the gray sequence is used in the center of the replacement window corresponding to the original grayscale of the pixel. This filtering method is nonlinear signal filtering, which can eliminate individual noise points and reduce the random impulse noise content in the image. We use the Canny operator edge detection method and area segmentation method to segment the filtered image.

The visual feature extraction method is used to carry out the distributed reorganization of the spatial information features of the regional 3D image, the edge contour feature extraction method is used to detect the boundary area of the regional 3D image, the spatially distributed reconstruction of the regional 3D image is carried out in the D-dimensional space, and the 3D model is combined with the construction method to establish a regional 3D image texture feature distribution set. When establishing the regional 3D image visual transmission model, it combines the fuzzy structure reorganization method to carry out the adaptive pixel reconstruction of the regional 3D image, the area where the visual information of the regional 3D image is reconstructed is S', the edge features are extracted in the edge contour part of the 3D image in the blurred area point (x', y'), the texture gradient is decomposed, and the texture distribution set of the 3D image in the blurred area is calculated. In the image registration process, the scale fixed feature transformation method is used to detect the extreme value by judging the space and judging the key point orientation and the main direction, determining the key point vector, and other processes describe and match the image corner feature.

The obtained corner point is taken as the optimal window center point of the Forstner operator, and the weighted centered corner point position is determined in the window. After determining the corner point features, it is necessary to use the distance between the corner points to match the feature points: preset a distance threshold, if the distance between the two corner points is less than this threshold, define the matching between the two corner points, and determine the relationship between the feature points in the two images based on this to achieve image registration. After defining the template feature distribution function for the super-resolution reconstruction of the 3D image of the region, we used the active contour detection method to reconstruct the 3D image feature of the fuzzy texture, then used the high-resolution region information fusion method to perform the feature decomposition of the 3D image of the fuzzy region, and extracted the 3D fuzzy region of image statistical feature components. Combining the edge contour feature extraction method to detect the boundary area of the regional three-dimensional image, we established the regional three-dimensional image visual transmission model and realized the design of the regional three-dimensional image visual transmission model.

## 4. Application and Analysis of the Regional 3D Image Virtual Model Based on Visual Communication Effect

4.1. Calibration of Image Preprocessing Parameters. Microsoft Visual C++ development tools and VTK 3D visualization toolkit are used as the design platform of a 3D image reconstruction system based on visual communication technology [5]. We use VC++ development tools to design system interfaces and write system integration and system core algorithms. The VTK 3D visualization toolkit kernel is developed by the Microsoft Visual C++ development tool and can be implemented on most platforms. The VTK 3D visualization toolkit, as a tool for the realization of visual communication technology, can realize the processing and visualization of 3D images [6]. This test builds a 3D reconstruction platform which is based on image editing tools, 3D production equipment, and professional engines. The C language is used as the platform to develop the language. The multiarchitecture network is used to transmit image data to ensure its timeliness and integrity. The editor selects highly integrated equipment to improve the running speed of reconstruction.

Aiming at the problem of dark images, we first perform histogram analysis and then use methods such as Gamma transformation and histogram equalization to improve the problem. From Table 2, we can see the comparison of 3D image reconstruction under different accuracy conditions of the gray level histogram which contains rich gray level information, reflects the gray level probability distribution of pixels, and is often used in spatial preprocessing, feature detection and matching. Gamma correction is a kind of nonlinear transformation, and its essence is to perform power exponential transformation on the gray value of the input image and then correct the brightness, which is mostly used to expand the details of the dark area. When the Gamma value is greater than 1, the dark part is expanded and the bright part is compressed; when the Gamma value is less than 1, the opposite is true. Histogram equalization is a common grayscale transformation method, which is simple and efficient to implement, and is widely used in image enhancement. Pixel grayscale changes randomly, resulting in uneven histogram height and uneven distribution. Under the condition that there is an intersection relationship between the boundary surface and a certain edge, considering the lack of a corresponding threshold value for the image, the intersection is implemented. The image is processed through histogram equalization to make the histogram roughly balanced and peaceful.

It can be seen from Figure 4 that the completeness of the reconstruction of the three-dimensional digital image using the system designed in this paper is significantly higher than that of the original system, and the completeness is relatively stable, while the original system fluctuates greatly. Through the comparison, it can be seen that the texture and color matching of the original system are quite different from the samples, and the reconstruction results in this paper are more consistent with the samples. It can be seen that the

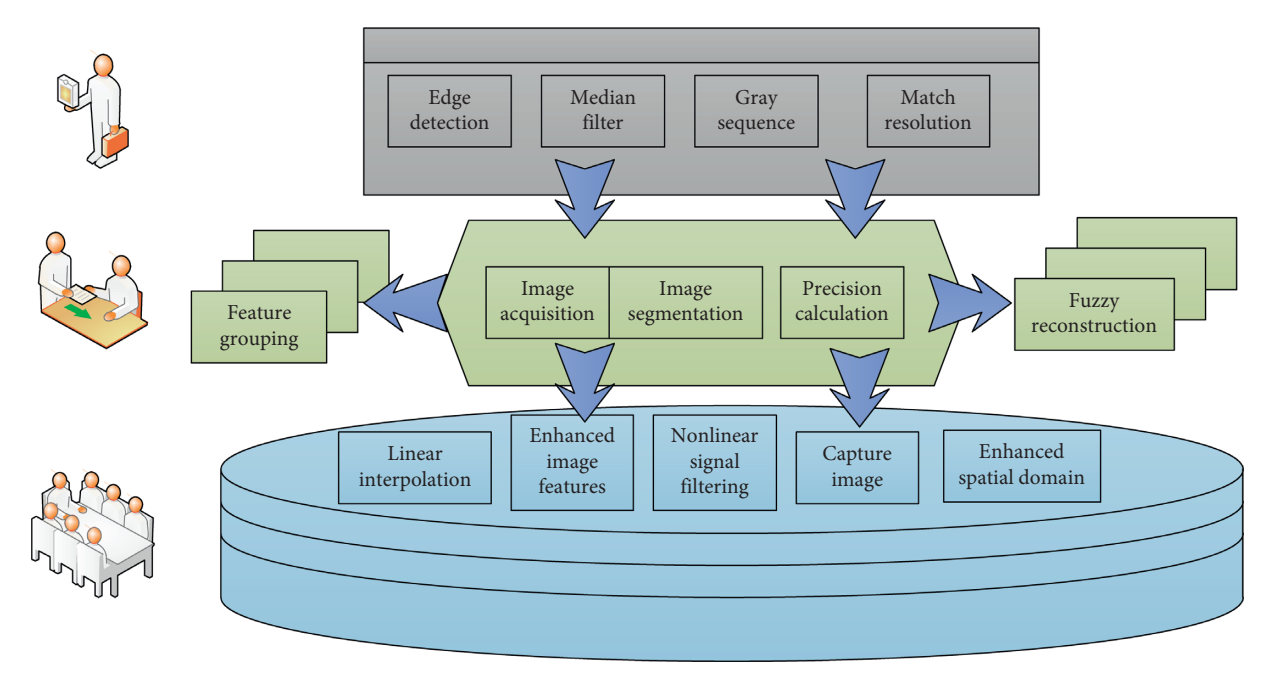


FIGURE 3: Frame diagram of the virtual reconstruction of 3D images based on visual communication.

Table 2: Comparison of 3D image reconstruction under different accuracy conditions.

Sample number	Image size	Resolution	Fitted value
1	$20 \times 30 \times 40$	350	0.98
2	$30 \times 40 \times 50$	300	0.99
3	$25 \times 35 \times 45$	250	0.97
4	$40 \times 50 \times 60$	220	0.98

performance and accuracy of the 3D digital image reconstruction system based on visual communication are better than the original system. At the same time, due to the high definition of the image used for 3D reconstruction, the error value is about 0.5 edge length, which is projected to reconstruction results.

4.2. 3D Image Feature Detection. According to the characteristics of the experimental scene, the camera was selected, and a mobile experimental platform was built on this basis. The software part uses VS2015+MFC, OpenCV, OpenGL, and other development software to integrate the implementation algorithms of each part. Finally, the 3D reconstruction effect is improved, and the reconstructed image is textured by Delaunay triangulation to improve the 3D reconstruction vision. As an image application library, the VTK 3D visualization toolkit visualization tool library is composed of three parts: computer image processing, visualization processing, and display. It has the characteristics of open source code, independent of operating system and hardware environment, and parallel processing. The threedimensional visualization VTK library includes a large number of high-quality image processing and generation algorithms. The VTK library is improved through the C++ language, and the visual communication technology is used achieve three-dimensional image reconstruction.

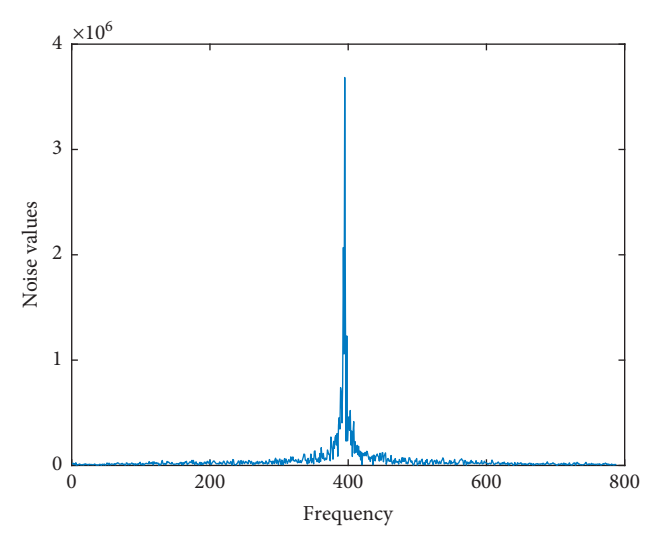


FIGURE 4: 3D image noise extraction spectrum.

According to the texture and detail area of the regional 3D image, the 3D texture structure reorganization and the sparse and scattered point reconstruction of the image are carried out, and the gray histogram of the 3D image of the region is reconstructed to obtain the *R*, *G*, and *B* components of the image W and the corresponding 3D image virtual reconstruction output feature distribution set AR, AG, AB and WR, WG, WB. Based on the above analysis, the virtual reconstruction of the regional 3D image is realized.

The realization of box filtering relies on the principle of integral image. In the fast solution of the integral image, the pixel value of the previous calculation in the rectangular frame is converted into the sum and difference of the corresponding corner points of the rectangular frame. Three-dimensional image information of different sample

points is shown in Figure 5. The image on the computer screen is basically the same as the image obtained by linear interpolation, so the midpoint of this edge is the intersection point. The most critical step of box filtering is to initialize the array S; each value in S is the sum of all pixels in the pixel neighborhood. Mean filtering is to use a template operator with the same weight to perform a convolution calculation on the entire area and output the convolution result. The common template cores are  $3 \times 3$  and  $7 \times 7$ . The effect of Gaussian filtering depends on the standard deviation, and its output is also a weighted average, but the weights are different from the mean filtering. The weights of the mean filtering are the same, while the weights of the Gaussian filtering are based on the distance between the points in the Gaussian kernel. The point distance is determined by the size' the smaller the distance is, the greater the weight is. Therefore, the Gaussian filtering effect is smoother and the edge information is better preserved. There are two ways to implement Gaussian filtering: discretization window convolution and benefit.

We use Fourier transform: the most commonly used is the first discrete window convolution. When the virtual reconstruction of the 3D image of the offset region is based on the MatLab simulation software, the matching template for the virtual reconstruction of the region 3D image is an 80×80 uniformly distributed template, which is the space for visual communication. The distribution area is  $2000 \times 2000$ , the learning rate of 3D image segmentation in the fuzzy area is 0.25, the number of randomly sampled pixels is 400, and the noise interference intensity is -12 dB. According to the above simulation parameter settings, the virtual reconstruction of the regional 3D image is performed. Taking the original brain MR image and heart CT image as examples, the image of attribute factors of different 3D image samples is shown in Figure 6. The analysis shows that the method in this paper can effectively realize the virtual reconstruction of 3D images and test the output signal-to-noise ratio. From the analysis of the comparison results, it can be seen that the output signal-to-noise ratio of the method in this paper is high, which improves the visual transmission effect of the reconstructed image.

4.3. Example Results and Analysis. The MicroBlaze softcore with a 32-bit microprocessor contains 32-bit general-purpose registers and 32-bit special registers, which have the advantages of low resource occupation and fast running speed. Among them, the special registers are the PC pointer and the MSR status flag register. Each interface of the MicroBlaze microprocessor is equivalent to a communication channel, with the characteristics of point-to-point single-item transmission, and can be directly connected to the FSL bus. The main function of the image analysis module is to provide support for different image data formats, based on which it completes the reading, conversion, and storage of data defined by the DICOM 3.0 standard. In the DICOM 3.0 standard, the image and related data transmission methods are designed in detail. Based on this standard, the Microsoft Visual C++ development tool and the VTK 3D

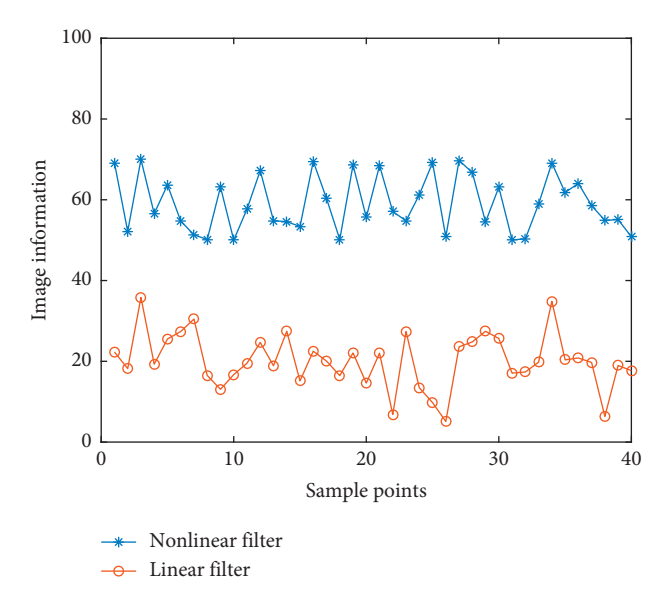


FIGURE 5: Three-dimensional image information of different sample points.

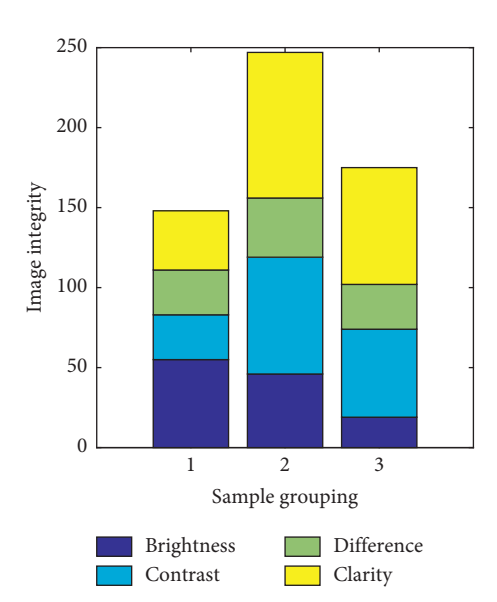


FIGURE 6: Histogram of attribute factors of different 3D image samples.

visualization toolkit are used to construct the required interfaces for the 3D image reconstruction system, and the image is transferred in the form of a VTK data stream. The information is converted into graphic data, which is convenient to realize the image adjustment of the dot matrix data, and the image data import processing is completed by relying on this interface. The histogram of the visual communication effect of the 3D image is shown in Figure 7. In order for the computer to recognize, we need to convert the feature information into the form of feature vectors. Each SIFT feature description point has 128 dimensions. The entire area is divided into 16 blocks, and each block is divided into 8 parts. For the experimental subjects in the previous experiment, the voxel division accuracy was set to

323, 1283, and 5123, and the image resolution was set to  $128 \times 128$ ,  $256 \times 256$ , and  $512 \times 512$ , respectively. The gradient direction of each part is counted. Each gradient direction contributes the same to the feature description, thus generating a rotationally invariant sum of the 128-dimensional feature vector of scale-invariant characteristics.

We compare the histogram of the original image of the human eye with the histogram of the noise simulation image, and the result is shown in Figure 8. Figure 8(a) is the original grayscale histogram of the human eye. The number of pixels in the grayscale area of [0.4, 0.75] is more distributed, showing a peak shape in [0, 0.3] and [0.7, 0.9]. The distribution of the number of pixels in the gray level area is less, showing a low valley shape. On the whole, the number of pixels is distributed in the gray level range of [0, 0.9], and the gray level increases. The number of pixels varies, and the overall appearance is jagged peaks and valleys. By separately describing the reconstruction time and speedup ratio of the system in this article and the 3D image reconstruction system based on RGB under different conditions, it can be obtained that the improvement of the voxel division accuracy leads to the extension of the 3D image reconstruction time of the two systems to varying degrees, and the speedup ratio varies with the body.

The details of the eyes and eyebrows are obvious in the image, which can be easily identified. Figure 8(b) is the image histogram after adding Gaussian noise. Compared with 8(a), it can be seen that it also shows peaks and valleys in [0.4, 0.75]. The number of pixels is more distributed, showing peak shape, and the number of pixels in the interval [0.0.3] and [0.8.1] is less distributed, showing a valley shape; but different from Figure 8(a), [0, 0.5]. In the interval, the trend of (b) map change is smoother than that of (a). In the interval [0.9], the number of pixels in (b) map is more than that. On the whole, (b) each gray of the change in the number of pixels within the degree level is gentle and uniform. This situation also reflects that the overall grayscale has not changed much, and the contrast of details is not strong enough, which is reflected in the blur and details of the noise brought by the image. Figure 8(c) is the image histogram after adding Poisson's noise. Whether it is the overall distribution or the peak-valley interval, it is similar to the original image. The difference is that the number of pixels in each gray level changes smoothly. The improvement in the accuracy of voxel division indicates that the 3D image reconstruction efficiency of the system in this paper is higher than that of the RGB-based 3D image reconstruction system, and with the improvement of the voxel division accuracy, the larger the acceleration ratio is, the more significant the acceleration effect is. The impact of this is that the contrast of image details is reduced, and the image appears overall blurry, but because its shape and value change little, it shows that the noise intensity in the image is

not large. It is the image histogram after adding salt and pepper noise. It is exactly the same as Figure 8(a) in the interval (0, 1), except that it appears at the two grayscale points of 0 and 1, respectively. The figure shows that the salt and pepper noise does not produce densely distributed noises like Gaussian noise and Poisson noise, nor does it blur the image as a whole, but it produces a considerable number of bright spots (white pixels) and dark points (black pixels 0), the energy is very large, and the noise points with great intensity appear in the image.

First, the corner points in the target image I1 and the image to be matched I2 are detected to form a set of characteristic corner points. Then, a point is selected from the feature corners of the image to be matched, and the feature corners of the target image are retrieved through the detection window. In fact, the NCC value of each point and the point to be matched is calculated to obtain a maximum point. Points are used as candidate points. Then, we perform a reverse search, select a corner point from the target image, and calculate the NCC value between the characteristic corner point of the image to be matched. When the NCC values of the characteristic corner points with a bidirectional relationship are greater than the set threshold, it means that the two characteristic corner points match. Compared with the NCC matching algorithm, the SSD matching algorithm is simpler in the description. It only needs to calculate the sum of squares of the gray difference between the target image and the feature point window function of the image to be matched to get the SSD value between the image point to be matched and the target point set. When the SSD value between the two points is the smallest, it is considered that they are matching point pairs. As can be seen from Figure 9, the median filter not only filters out random noise points well but also preserves image details well. In median filtering, noise is often arranged at both ends of the entire template area and has almost no effect on the output result, while average filtering is a way of calculating the average to get the output, and noise has a greater impact on its output. Therefore, the median filtering effect is better in filtering random noise, and it is a better nonlinear filtering method. A high-quality 3D image reconstruction system must ensure high reconstruction accuracy while ensuring high reconstruction efficiency. It describes the reconstruction accuracy and image clarity of the experimental objects for the reconstruction of the two systems. Analyzing it, the accuracy of reconstructing 3D images of objects using this system is higher than 95%, the reconstruction accuracy and clarity are significantly higher than that of RGB-based systems, and the reconstruction accuracy of tooth images is higher than that of mountain images, indicating that this system can accurately reconstruct the three-dimensional image of the object, and the smaller the image is, the higher the reconstruction accuracy is.

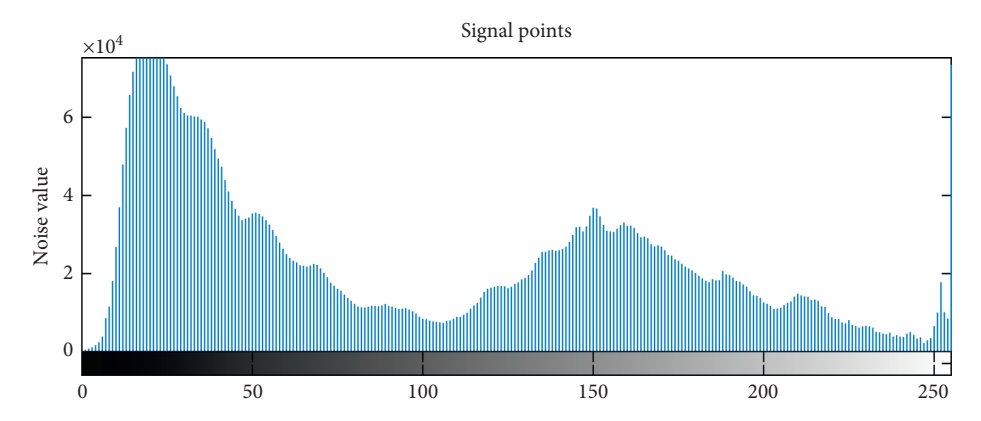


FIGURE 7: Histogram of visual communication effect of the 3D image.



FIGURE 8: Visual communication effect after filtering processing of the 3D image. (a) Original image. (b) Salt and pepper noise. (c) Gaussian noise.

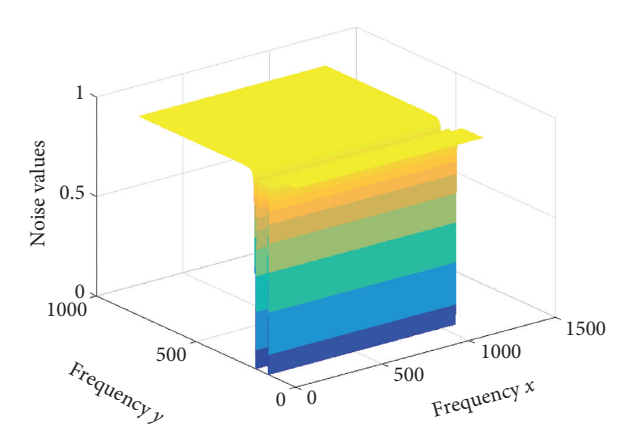


FIGURE 9: Three-dimensional perspective view of the filtered three-dimensional image.

## 5. Conclusion

This paper uses the Microsoft Visual C++ development tool and VTK 3D visualization toolkit as the design platform to design a 3D image reconstruction system of visual communication technology composed of an image analysis

module, image preprocessing module, and 3D visualization module. In the process of 3D image reconstruction, 3D volume rendering and surface rendering of the object in the 3D visualization module are more important. The volume rendering image and the surface rendering image are combined to form a 3D reconstruction image of the object.

Therefore, the 3D reconstruction image depends on the rendering accuracy of the two. In the follow-up research process, we can focus on the process of volume rendering and surface rendering to improve the system's 3D image reconstruction accuracy. We construct the grid distribution model of the regional three-dimensional image, use the visual feature extraction method to carry out the distributed reorganization of the spatial information feature of the regional three-dimensional image, and combine the edge contour feature extraction method to detect the boundary area of the regional three-dimensional image. We establish a visual communication model of the regional 3D image, combine the fuzzy structure reconstruction method to carry out the adaptive pixel reconstruction of the regional 3D image, carry out the 3D texture structure reconstruction of the image according to the texture and detail area of the regional 3D image, and reconstruct the sparse and scattered points to reconstruct the regional 3D image. The grayscale histogram is based on the visual communication effect to realize the virtual reconstruction of the regional three-dimensional image. The simulation results show that the visual effect of the virtual reconstruction of the regional 3D image using this method is better, and the quality of the 3D image virtual reconstruction is higher.

## **Data Availability**

The data used to support the findings of this study are available from the corresponding author upon request.

## **Conflicts of Interest**

The authors declare no conflicts of interest.

#### References

- [1] J. Feng, Q. Teng, B. Li et al., "An end-to-end three-dimensional reconstruction framework of porous media from a single two-dimensional image based on deep learning," *Computer Methods in Applied Mechanics and Engineering*, vol. 368, pp. 11–30, 2020.
- [2] T. F. Chen-Yoshikawa and H. Date, "Update on three-dimensional image reconstruction for preoperative simulation in thoracic surgery," *Journal of Thoracic Disease*, vol. 8, no. Suppl 3, p. S295, 2018.
- [3] M. A. Sutton, S. R. McNeill, J. D. Helm et al., "Advances in two-dimensional and three-dimensional computer vision," *Photomechanics*, vol. 77, no. 1, pp. 323–372, 2000.
- [4] V. Murino and A. Trucco, "Three-dimensional image generation and processing in underwater acoustic vision," *Proceedings of the IEEE*, vol. 88, no. 12, pp. 1903–1948, 2020.
- [5] J. J. Atick, P. A. Griffin, and A. N. Redlich, "Statistical approach to shape from shading: reconstruction of three-dimensional face surfaces from single two-dimensional images," *Neural Computation*, vol. 8, no. 6, pp. 1321–1340, 2019.
- [6] A. Stern and B. Javidi, "Three-dimensional image sensing, visualization, and processing using integral imaging," *Proceedings of the IEEE*, vol. 94, no. 3, pp. 591–607, 2018.
- [7] R. Klette, A. Koschan, and K. Schluns, *Three-Dimensional Data From Images*, vol. 4, pp. 21–28, Springer-Verlag Singapore Pte. Ltd., Singapore, 2018.

[8] J. Huo and X. Yu, "Three-dimensional mechanical parts reconstruction technology based on two-dimensional image," *International Journal of Advanced Robotic Systems*, vol. 17, no. 2, pp. 17–28, 2020.

- [9] G. Verhoeven, "Taking computer vision aloft–archaeological three-dimensional reconstructions from aerial photographs with photoscan," *Archaeological Prospection*, vol. 18, no. 1, pp. 67–73, 2021.
- [10] T. Xue, L. Qu, Z. Cao et al., "Three-dimensional feature parameters measurement of bubbles in gas-liquid two-phase flow based on virtual stereo vision," *Flow Measurement and Instrumentation*, vol. 27, pp. 29–36, 2019.
- [11] S. Liu, L. Zhao, and J. Li, "The applications and summary of three dimensional reconstruction based on stereo vision," in Proceedings of the 2012 International Conference on Industrial Control and Electronics Engineering, pp. 620–623, Xi'an, China, 2012.
- [12] J. A. Gibbs, M. Pound, A. P. French, D. M. Wells, E. Murchie, and T. Pridmore, "Approaches to three-dimensional reconstruction of plant shoot topology and geometry," *Functional Plant Biology*, vol. 44, no. 1, pp. 62–75, 2017.
- [13] G. Xu, X. Li, J. Su et al., "Precision evaluation of three-dimensional feature points measurement by binocular vision," *Journal of the Optical Society of Korea*, vol. 15, no. 1, pp. 30–37, 2021.
- [14] T. Leung and J. Malik, "Representing and recognizing the visual appearance of materials using three-dimensional textons," *International Journal of Computer Vision*, vol. 43, no. 1, pp. 29–44, 2020.
- [15] J. De Reu, G. Plets, G. Verhoeven et al., "Towards a three-dimensional cost-effective registration of the archaeological heritage," *Journal of Archaeological Science*, vol. 40, no. 2, pp. 1108–1121, 2018.
- [16] K. J. Park, C. J. Bergin, and J. L. Clausen, "Quantitation of emphysema with three-dimensional CT densitometry: comparison with two-dimensional analysis, visual emphysema scores, and pulmonary function test results," *Radiology*, vol. 211, no. 2, pp. 541–547, 2019.
- [17] E. N. Leith and J. Upatnieks, "Wavefront reconstruction with diffused illumination and three-dimensional objects," *Josa*, vol. 54, no. 11, pp. 1295–1301, 2019.
- [18] Y. Tang, M. Chen, Y. Lin et al., "Vision-based three-dimensional reconstruction and monitoring of large-scale steel tubular structures," *Advances in Civil Engineering*, vol. 2, pp. 12–18, 2020.
- [19] G. Plets, G. Verhoeven, D. Cheremisin et al., "The deteriorating preservation of the Altai rock art: assessing three-dimensional image-based modelling in rock art research and management," *Rock Art Research: The Journal of the Australian Rock Art Research Association (AURA)*, vol. 29, no. 2, pp. 139–156, 2019.
- [20] F. Yao, J. Wang, J. Yao, F. Hang, X. Lei, and Y. Cao, "Three-dimensional image reconstruction with free open-source OsiriX software in video-assisted thoracoscopic lobectomy and segmentectomy," *International Journal of Surgery*, vol. 39, pp. 16–22, 2017.
- [21] M. Xu, C. Li, Z. Chen et al., "Assessing visual quality of omnidirectional videos," *IEEE Transactions on Circuits and Systems for Video Technology*, vol. 29, no. 12, pp. 3516–3530, 2018.
- [22] M. Yang and A. Sowmya, "An underwater color image quality evaluation metric," *IEEE Transactions on Image Processing*, vol. 24, no. 12, pp. 6062–6071, 2015.

[23] Q. Jiang, F. Shao, W. Lin et al., "Optimizing multistage discriminative dictionaries for blind image quality assessment," *IEEE Transactions on Multimedia*, vol. 20, no. 8, pp. 2035–2048, 2017.

- [24] C. Chen, K. Li, W. Wei, J. T. Zhou, and Z. Zeng, "Hierarchical graph neural networks for few-shot learning," *IEEE Transactions on Circuits and Systems for Video Technology*, p. 1, 2021.
- [25] W. Wei, X. Fan, H. Song, and H. Wang, "Video tamper detection based on multi-scale mutual information," *Multi-media Tools and Applications*, vol. 78, no. 19, pp. 27109–27126, 2019
- [26] J. Yang, C. Wang, B. Jiang et al., "Visual perception enabled industry intelligence: state of the art, challenges and prospects," *IEEE Transactions on Industrial Informatics*, vol. 17, no. 3, pp. 2204–2219, 2020.
- [27] Y. Li, J. Nie, and X. Chao, "Do we really need deep CNN for plant diseases identification?" *Computers and Electronics in Agriculture*, vol. 178, p. 105803, 2020.
- [28] M. Chen, S. Lu, and Q. Liu, "Uniqueness of weak solutions to a Keller-Segel-Navier-Stokes system," *Applied Mathematics Letters*, vol. 121, Article ID 107417, 2021.
- [29] J. Yang, M. Xi, B. Jiang et al., "FADN: fully connected attitude detection network based on industrial video," *IEEE Trans*actions on Industrial Informatics, vol. 17, no. 3, pp. 2011–2020, 2020.
- [30] M. P. Heinrich, O. Oktay, and N. Bouteldja, "OBELISK-Net: fewer layers to solve 3D multi-organ segmentation with sparse deformable convolutions," *Medical Image Analysis*, vol. 54, pp. 1–9, 2019.